Magnetic structure and field-dependent magnetic phase diagram of Ni_2In-type PrCuSi

Harikrishnan S. Nair[1], C. M. N. Kumar[2], D. T. Adroja[3,4], C. Ritter[5], A. S. Wills[6], W. A. Kockelmann[4], Pascale P. Deen[7,8], A. Bhattacharyya[4,9] A. M. Strydom[3,10]

[1]Department of Physics, 500 W. University Ave, University of Texas at El Paso, TX 79968, USA

[2]Institut für Festkörperphysik, TU Wien, Wiedner Hauptstr. 8-10/138, 1040 Wien, Austria

[3]Highly Correlated Matter Research Group, Department of Physics, University of Johannesburg, P.O. Box 524, Auckland Park 2006, South Africa

[4]ISIS Facility, STFC, Rutherford Appleton Laboratory, Chilton, Didcot, Oxfordshire OX11 0QX, United Kingdom

[5]Institut Laue-Langevin, 71, Avenue des Martyrs, Grenoble 38000, France

[6]Department of Chemistry, University College London, 20 Gordon Street, London, WC1H 0AJ, United Kingdom

[7]Nanoscience Center, Niels Bohr Institute, University of Copenhagen, DK-2100 Copenhagen, Denmark

[8]European Spallation Source, Tunavägen 24, Lund, Sweden

[9]Department of Physics, Ramakrishna Mission Vivekananda Educational and Research Institute, PO Belur Math, Howrah 711202, West Bengal, India

[10]Max Planck Institute for Chemical Physics of Solids (MPICPfS), Nöthnitzerstraße 40, 01187 Dresden, Germany

E-mail: h.nair.kris@gmail.com and hnair@utep.edu

Abstract. The magnetic structure of the ternary equiatomic intermetallic compound PrCuSi is investigated using neutron powder diffraction experiments in 0 T as well as in external magnetic fields up to 2 T. The PrCuSi compound crystallizes in the hexagonal Ni_2In-type structure, in the space group $P6_3/mmc$. In this structure, cationic ordering of Cu and Si takes place. The antiferromagnetic phase transition in the Pr sublattice takes place at $T_N = 5.1$ K in 0 T. Under an external magnetic field of 2 T, a field-induced ferromagnetic phase is observed. Magnetoelastic coupling is evidenced by an increase in the unit cell volume. Clear signatures of a mixed antiferromagnetic and ferromagnetic phase in weak, intermediate fields, 0.4–0.8 T, are obtained from the present study. Using the present set of experimental data, we construct the H–T phase diagram of PrCuSi.

Keywords: PrCuSi, magnetostructural effect, antiferromagnet, field-induced, ferromagnetism

PACS numbers:

Submitted to: *J. Phys.: Condens. Matter*

1. Introduction

The ternary equiatomic RTX are series of compounds where R is a rare earth, T is a transition metal and X is a main group (IIIB or IVB) element [1]. Despite their chemical simplicity, they exhibit structurally and magnetically diverse properties that have recently been reviewed in Ref. [2]. This renewed interest in the RTX compounds is due to the observation of the magnetocaloric effect and magnetoresistance [3, 4]. The RTX compounds display a very wide range of magnetic ordering temperatures ranging from a few Kelvin to above room-temperature, making them suitable for magnetocaloric applications across a wide temperature range. Copper-based RCuSi and RCuGe compounds in the hexagonal AlB_2-type crystal structure were reported very early in the literature [5, 6] and several other compounds with X = Ga, Si or Ge, and T = Cu, Rh, Pd were investigated to study the crystal structure [7]. Careful heat treatment of RCuSi compounds leads to a fully ordered atomic arrangement of the three elements R, Cu, and Si. In general, the disordered high temperature phase belongs to the $P6/mmm$ hexagonal space group (AlB_2-type structure), whereas the low temperature ordered modification is the $P6_3/mmc$ with Ni_2In-type structure [6]. In the disordered $P6/mmm$ space group, T and X atoms are randomly distributed over $2d$ sites while R occupies the $1a\,(000)$ Wyckoff position. In the ordered case, T and X occupy $2c\left(\frac{1}{3}\frac{2}{3}\frac{1}{4}\right)$ and $2d\left(\frac{1}{3}\frac{2}{3}\frac{3}{4}\right)$ positions and R the $2a(000)$ position. As a consequence of ordering among T and X, the unit cell of the $P6_3/mmc$ structure is doubled along the c-axis [6]. This type of hexagonal structure is characterized by plane layers of hexagons formed by alternating Si and Cu atoms stacked in such a way that a Cu atom alternates with a Si atom in the subsequent layer and vice versa. Each Cu (Si) atom has three Si (Cu) atoms as nearest neighbours in the same layer. The rare earth atoms are located between two hexagonal layers. A schematic diagram of the unit cell of PrCuSi is presented in Fig 1 (a) and the hexagonal layered structure of Cu/Si atoms and the Pr atoms that occupy the space between the layers are shown as a projection on to the ab-plane in panel (b).

The magnetic structure of RCuSi compounds depends on the type of rare earth at the R site [8]. The heavier Rs, which have well-localized spins, form complex spin arrangements in RCuSi. Transverse sine wave modulated antiferromagnetic ordering is observed in TbCuSi (T_N = 16 K) [8], DyCuSi (T_N = 11.9 K) [9] and HoCuSi (T_N = 9.5 K) [9]. Modulated type of ordering is observed in ErCuSi [10] with a T_N = 6.8 K which squares up below 3.5 K. In the case of TmCuSi, a sine wave modulated phase is formed at T_N = 6.5 K which develops into ferromagnetic ordering below 5.8 K [11]. In contrast, with the lighter rare earth member Ce, CeCuSi is a ferromagnet with T_c = 15.5 K [12, 13]. Earlier investigations on GdCuSi in the AlB_2 structure identified it as a ferromagnet with a relatively high T_c of 49 K [14]. In comparison, recent studies on GdCuSi in the Ni_2In-type structure identified an antiferromagnetic transition at T_N = 14.2 K with a spin re-orientation transition further below near 5 K [15]. A significant magnetocaloric effect with $-\Delta S_m \approx 8$ J/mol K at 5 T is reported for GdCuSi [15]. In the

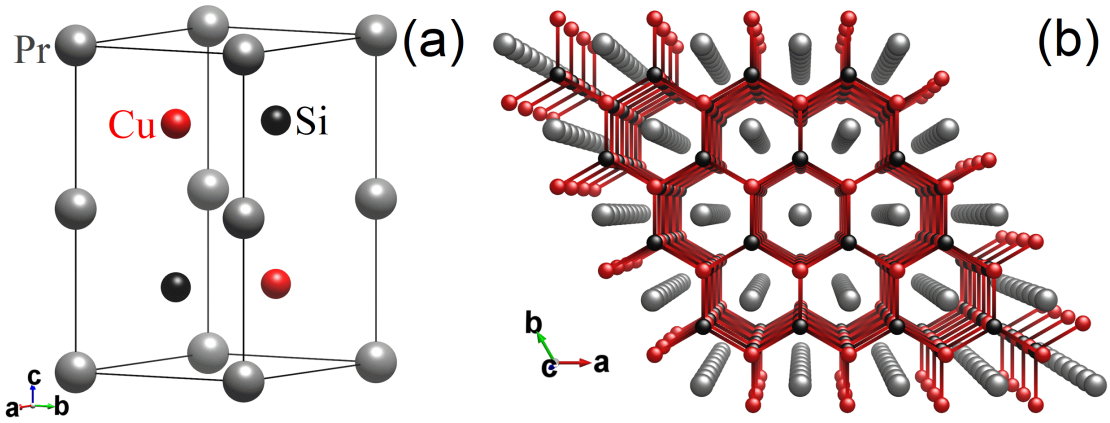

Figure 1. (color online) A schematic diagram of the hexagonal $P6_3/mmc$ structure (Ni_2In type) of PrCuSi. (a) The unit cell of PrCuSi with Pr represented as the gray spheres, the red are Cu and the black spheres are Si. (b) The hexagonal layered network formed by the Cu and Si atoms.

case of NdCuSi, mixed antiferromagnetic and ferromagnetic ordering is reported to occur at low temperature [16], which leads to the observation of a significant magnetocaloric effect and magnetoresistance. The earliest work on PrCuSi by Oesterreicher identified it as a ferromagnet with Curie temperature $T_c \approx 14$ K[14]. It should be noted that the PrCuSi that they studied was in the AlB_2-type structure which has the disordered space group $P6/mmm$. Also, the ordered moment in the ferromagnetic region was found to be reduced compared to the theoretical value. The motivation for Oesterreicher's early work was to investigate the competition between the crystalline electric field and the magnetic exchange that leads to magnetic ordering.

Several layered intermetallic compounds similar to the present layered PrCuSi, or intermetallics with the propensity of forming structurally mixed phases, display magnetoelastic coupling which is tapped for useful properties like magnetocaloric effect or magnetoresistance. The magnetocaloric material $Gd_5Si_2Ge_2$ is one such compound where structural instability in the presence of a magnetic field leads to a giant magnetocaloric effect [17, 18]. Similarly, the $R_2Mn_2Ge_2$ compounds are another example where field-induced changes in the lattice constants and unit cell volume gave strong indication of the magnetoelastic coupling as a consequence of different structural components having ferromagnetic and antiferromagnetic regions [19, 20, 21, 22]. The Heusler alloys are another important class of intermetallics that display very similar magnetostructural effects leading to magnetoresistance [18]. In the present compound, PrCuSi, we observe strong evidence of a magnetostructural effect under applied magnetic field, which comes from our neutron diffraction results. In the context of the magnetocaloric effect reported recently in the case of GdCuSi and NdCuSi[15, 16], our result of magnetostructural effect in PrCuSi assumes greater importance.

In the present paper, we investigate the magnetic structure of PrCuSi using neutron powder diffraction in zero and applied magnetic fields. We observe an antiferromagnetic phase transition in the Pr magnetic lattice at 5 K (at variance with the earlier work that reports ferromagnetic ordering at T_c = 14 K[14]) which transforms into a ferromagnetic phase with the application of 2 T. Significant field-induced magnetoelastic coupling is experimentally observed in PrCuSi through the present study. Paramagnetic, antiferromagnetic and the field-induce ferromagnetic phases are identified in the H–T phase diagram, in addition to a mixed (AFM + FM) phase in low fields.

2. Experimental details

Polycrystalline powder samples of PrCuSi, weighing about 15 g, used in the present neutron investigation were prepared using an arc melting method reported elsewhere [23]. Magnetization, specific heat and electrical transport of PrCuSi are reported in a previous publication [23]. The polycrystalline samples were magnetically characterized to identify the magnetic phase transition temperature before performing the neutron scattering experiments. Neutron powder diffraction experiments on PrCuSi were performed at two instruments, *viz.,* the constant wavelength diffractometer D2B at Institut Laue Langevin, Grenoble, and the time-of-flight (TOF) spectrometer GEM at the ISIS facility, Rutherford Appleton Laboratory, UK. Diffraction data on D2B were collected in 0 T as well as in 0.5 T and 2 T in order to elucidate the magnetic structure and to validate the phase diagram that was estimated in Reference [23]. For the experiment at D2B, λ = 1.594 Å was the selected wavelength. The powder sample that was measured under field was soaked in deuterated isopropanol which gets solid at low temperatures and hinders the powder grains from aligning in the magnetic field. At GEM, several 6-banks of data were collected at each temperature to cover a large d-range. The diffraction data was analyzed using the Rietveld method [24] in the software FullProf Suite [25]. The irreducible representations of magnetic structures were determined using the software SARAh [26].

3. Results and discussion

In this section we first discuss the analysis of neutron powder diffraction data obtained on PrCuSi at $T > T_N$ = 5.1 K with the aim of elucidating the crystal structure in the paramagnetic regime. The neutron diffraction data at $T > T_N$ were collected at the TOF spectrometer GEM. In Fig 2, the experimentally obtained diffracted intensity for (a) 300 K and (b) 20 K respectively (data from only one bank is presented) are presented using black circles as markers. As discussed in Section 1, the crystal structure of PrCuSi was first studied in the structure type AlB_2 [14]. However, there are several RCuSi compounds that adopt the Ni_2In-type structure. Hence the first step was to estimate the correct structure type for the PrCuSi samples used in the present study. We performed Rietveld analysis of the experimental neutron diffraction pattern and consequently the

pattern at 300 K was refined using the structural model of the hexagonal space group, $P6_3/mmc$ (Ni_2In-type) which allows for cationic ordering. In addition to this majority hexagonal phase, a minority phase of the disordered $P6/mmm$ (AlB_2-type) was also observed. At 300 K, the ratio $P6_3/mmc$:$P6/mmm$ of the two phases obtained through refinement was 96%:4% by weight. In Fig 2, the calculated diffraction pattern using the two-phase model is shown as red solid line. The allowed Bragg peaks for the two different phases are shown in the figure as vertical bars – the top set for the major phase ($P6_3/mmc$) and the lower one for the minor phase ($P6/mmm$). There is no structural phase transition observed in PrCuSi as a function of temperature and the phase fractions of the $P6_3/mmc$ and $P6/mmm$ phases remain in the same ratio down to 20 K. At 300 K, the refined values of lattice parameters for the major phase are a = 4.222(4) Å and c = 7.906(5) Å. These values are comparable to the values of PrCuSi reported in a study on a series of RCuSi compouds that adopt the Ni_2In-type structure [6]. Our Rietveld refinements confirm that PrCuSi adopts the Ni_2In-type structure with a doubled unit cell along the c-axis as a consequence of atomic ordering of Cu and Si. However, the presence of the disordered $P6/mmm$ phase is clear in the diffraction patterns (indicated by the lower set of vertical tick marks in Fig 2). For example, the peak in Fig 2 (a) that occurs at $d \approx 1.45$ Å is accounted for only by the minority phase of PrCuSi in the space group $P6/mmm$. Binary phases of Pr, Cu and Si were ruled out in the present case. In Table 1, the refined values of the lattice constants for 300 K, 20 K and 10 K are presented. Also provided are the atomic coordinates of the majority and the minority phases of PrCuSi structure ($P6_3/mmc$ and $P6/mmm$ respectively). It can be seen that the majority phase is an ordered structure whereas in the case of the minority phase, Cu and Si are disordered. In the structural refinement cycles, the occupancy of Pr was fixed and then those of Cu and Si were varied. In the case of the auxiliary phase, all the occupancies were fixed to the theoretical value defined as occupancy = (site occupancy/general occupancy).

Contrary to the early report on PrCuSi in the AlB_2-type which reported a magnetic phase transition at the Curie temperature, T_c = 14 K [14], our diffraction data do not support long-range ordered magnetic state for PrCuSi down to 5 K. Refer panel (c) of Fig 2 where the diffraction pattern obtained at 10 K from the instrument D2B is shown. It can be seen that the observed reflections are completely accounted for by the nuclear space group of the majority phase of PrCuSi ($P6_3/mmc$) and the secondary nuclear phase ($P6/mmm$) corresponding to the impurity phase of disordered PrCuSi. Some of the observed reflections in the figure are shown indexed in the space group $P6_3/mmc$. From the diffraction data obtained at $T \geq$10 K, it is clear that no long-range magnetic order in PrCuSi develops at 14 K. To probe the magnetic order at low temperature we collected neutron diffraction data at $T < 6$ K. In order to track the magnetic phase transition and to observe the temperature dependence of magnetic moment at low temperatures, we obtained neutron diffraction patterns at 13 temperature points between 1.5 K and 5.4 K. Compared to the diffraction patterns obtained in the temperature range 10 K – 300 K, the diffraction pattern at 2 K showed additional

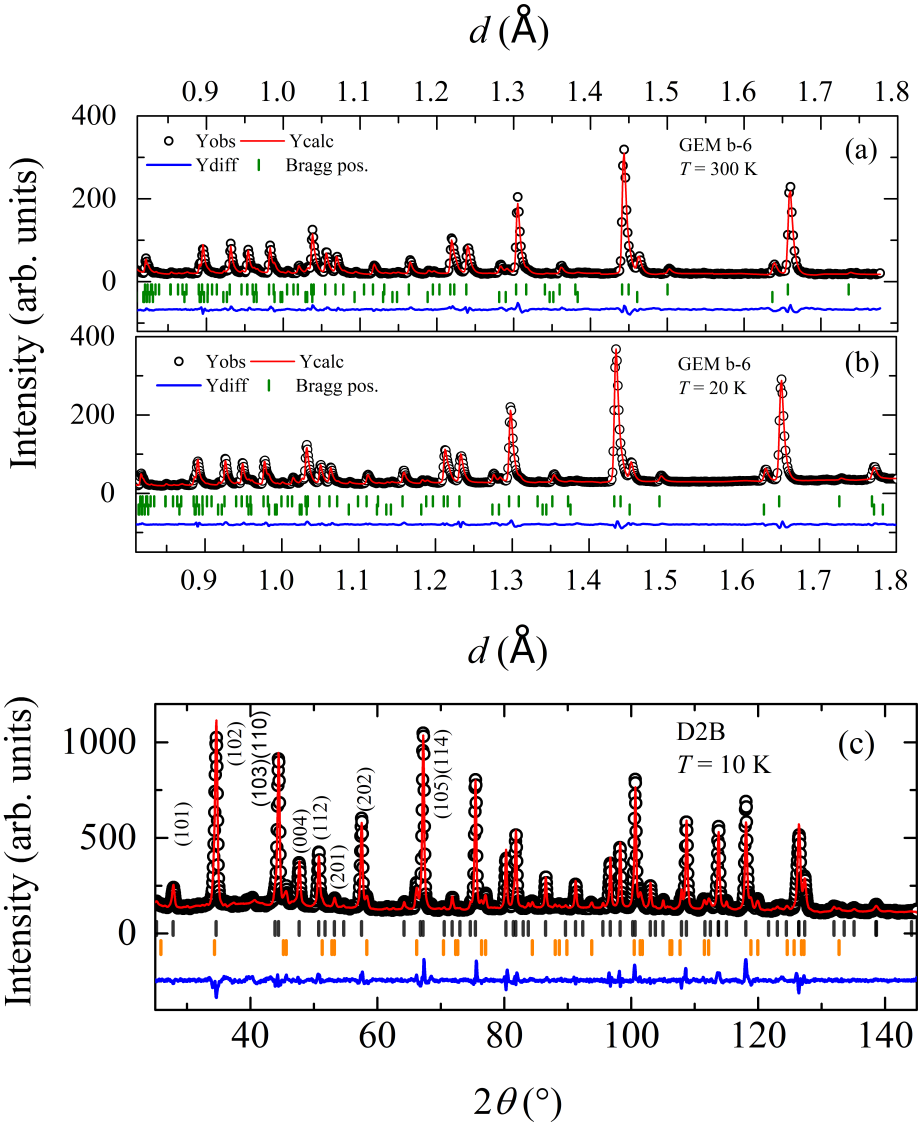

Figure 2. (color online) The experimental neutron powder diffraction patterns of PrCuSi at (a) 300 K and (b) 20 K along with Rietveld refinement fits. The refinement used a mixed-structural model using the space group $P6_3/mmc$ as a majority phase (96%) and $P6/mmm$ as a minority phase (4%). As indicated in the figure, the upper set of Bragg peaks indicate the majority phase and lower set, the minority phase. (c) Shows the refined diffraction pattern of PrCuSi at $T = 10$ K (below the T_N reported in Ref. [14]) confirming the absence of magnetic order.

peaks at $2\theta \approx 26.5°$, $32.1°$, $41.3°$, which we attribute to magnetic order. However, no significant enhancement in the intensities of the diffraction peaks were observed on cooling from 10 K to 2 K. Our previous magnetometry study indicated a magnetic phase transition in PrCuSi at $T_N = 5.1$ K that was characterized antiferromagnetic as the peak in the magnetization was not shifted by low applied fields, along with the field-independence of the slope of magnetization [23]. The antiferromagnetic transition was confirmed also from the negative Curie-Weiss temperature, $\theta = -4.11(4)$ K. Thus,

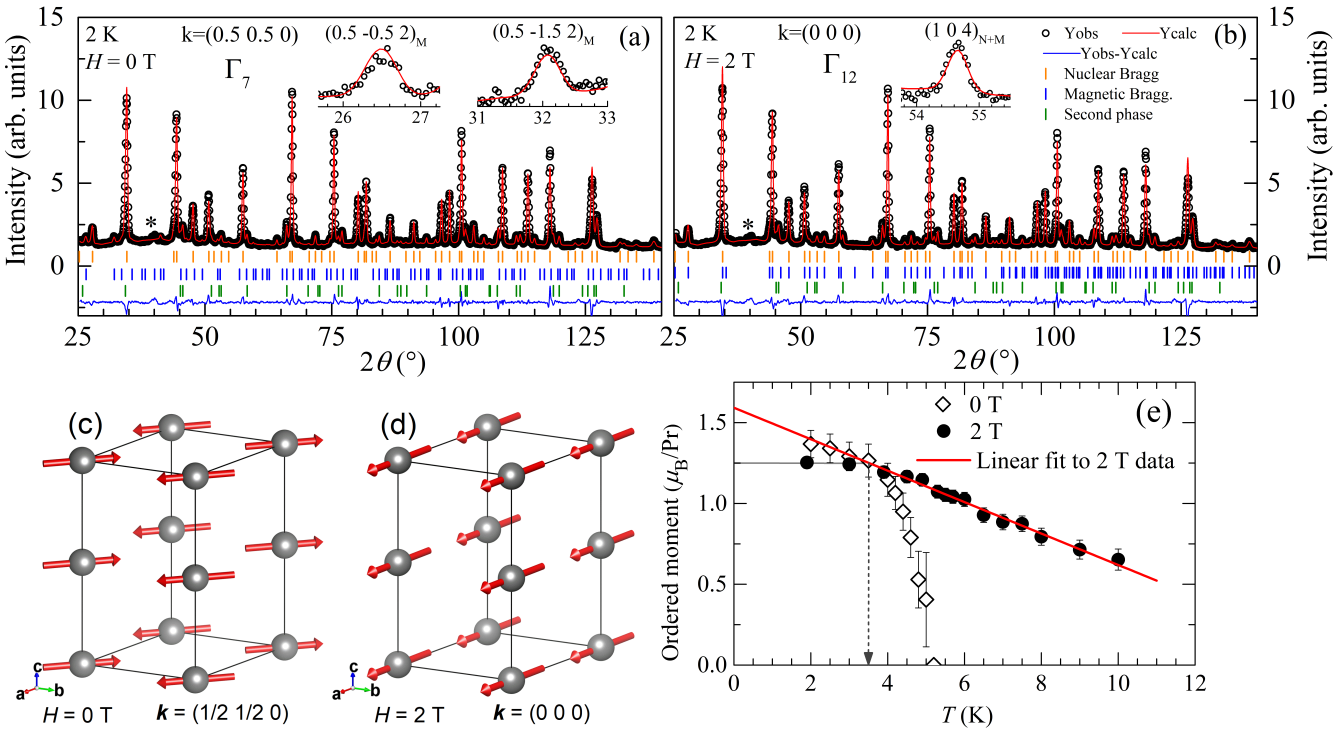

Figure 3. (color online) (a) The experimentally obtained neutron powder diffraction patterns of PrCuSi at 2 K under zero applied field (H = 0 T). The red solid line is the calculated pattern using the magnetic structure model of reprepsentation, Γ_7. The magnetic propagation vector was k = ($\frac{1}{2}$ $\frac{1}{2}$ 0). (b) The diffracted intensity at 2 K under a magnetic field of 2 T. The magnetic structure was solved using the Γ_{12} representation with the propagation vector, k = (0 0 0). An unknown minor impurity peak is indicated by an asterisk in (a) and (b). (c) The magnetic structure (Γ_7) at T = 2 K under H = 0 T and (d) (Γ_{12}) under H = 2 T. (e) The temperature dependence of the refined magnetic moment displays the order parameter for H = 0, 2 T confirming T_N = 5.1 K for H = 0 T.

the zero-field magnetic state of PrCuSi was ascertained as antiferromagnetic rather than ferromagnetic as per the previous report.

Figure 3 shows the diffraction patterns at 2 K obtained in (a) zero field, H = 0 T and at (b) H = 2 T. The nuclear structure at 2 K was refined using the two-phase structural model that was previously used for 300 K data. The majority phase of $P6_3/mmc$ and minority phase of $P6/mmm$ were identified at 2 K also. The top two rows of Bragg peaks (the vertical ticks in the figure) correspond to these two structural phases. Quantitative estimation of the volume fraction of these phases showed that the majority phase fraction was ≈ 96%. In order to determine the magnetic structure at H = 0 T, the k vector (magnetic propagation vector) was determined using the k-search utility within the FullProf suite. k = ($\frac{1}{2}$ $\frac{1}{2}$ 0) was obtained as the best solution and was used as input in the software SARAh [26] to obtain the irreducible magnetic representation for PrCuSi. Among four allowed irreducible representations, the AFM

representation Γ_7 (in Kovalev's notation) was adjudged the best fit for the observed magnetic intensities through Rietveld fits. In Fig 3 (a) the red solid line represents the calculated diffraction pattern using the magnetic structure Γ_7. In the inset of (a), two purely magnetic reflections ($\frac{1}{2}$ -$\frac{1}{2}$ 2) and ($\frac{1}{2}$ -$\frac{3}{2}$ 2) are presented along with the fits according to the Γ_7 model. The arrangement of the spins as per the magnetic model is shown schematically in (c) for the zero-field case. It constitutes an overall antiferromagnetic structure with a ferromagnetic alignment of spins along the c-axis where the chains themselves align antiferromagnetically. In order to show clearly the differences between the allowed irreducible representations, we present the refinement of the neutron diffraction data using all the four representations – Γ_1, Γ_3, Γ_5 and Γ_7 – in figure 4. In the figure, the refinements obtained at $T = 2$ K and $H = 0$ T are shown in the 2θ range 25° to 35° where the major magnetic reflections are present. It can be seen from the visual quality of the fit, that the Γ_7 representation is the best description for the magnetic structure of PrCuSi at 0 T. The goodness–of–fit values for the magnetic refinement (magnetic R-factors) obtained for the fits are as follow: Γ_1 (33), Γ_3 (33), Γ_5 (22.5) and Γ_1 (13).

With the application of a magnetic field at $H = 2$ T, no new magnetic Bragg peaks are observed to emerge. However, a significant intensity variation was observed at the nuclear Bragg peaks, indicating a field induced magnetic phase transition with the propagation vector $k = (0\ 0\ 0)$. Among the 4 possible irreducible representations suggested by symmetry, we found ferromagnetic representation (Γ_{12}) as the best fit for the experimental data. In panel (b) of Fig 3, the red solid line represents the calculated intensity as per this model. The inset of (b) shows a combined nuclear/ magnetic reflection along with the fitted curve. The magnetic structure of PrCuSi

Table 1. The refined lattice parameters of PrCuSi at 300 K and at 20 K after Rietveld analysis of the neutron diffraction data obtained from the instrument GEM. The parameters pertaining to the major hexagonal phase of $P6_3/mmc$ and the $P6/mmm$ minority phase are given. The space group and the atomic coordinates of the majority and minority phases are given. The minority phase was in all cases always less that $\approx 4\%$. The parameters pertaining to 10 K are obtained from the experiment at D2B, Grenoble. The atomic positions are, Pr(2a) (000); Cu (2c) ($\frac{1}{3}$ $\frac{2}{3}$ $\frac{1}{4}$); Si (2d) ($\frac{1}{3}$ $\frac{2}{3}$ $\frac{3}{4}$) in the $P6_3/mmc$ setting and Pr(2a) (000); Cu (2c) ($\frac{1}{3}$ $\frac{2}{3}$ $\frac{1}{2}$); Si (2d) ($\frac{1}{3}$ $\frac{2}{3}$ $\frac{1}{2}$) in the $P6/mmm$ case.

$P6_3/mmc$ (96% wt.)			
	300 K	20 K	2 K
$a(\AA)$	4.2212(4)	4.2123(7)	4.2061(4)
$c(\AA)$	7.9051(2)	7.8858(8)	7.8693(2)
$P6/mmm$ (4% wt.)			
	300 K	20 K	2 K
$a(\AA)$	4.1176(4)	4.1092(2)	4.1007(4)
$c(\AA)$	4.1553(2)	4.1464(3)	4.1410(2)

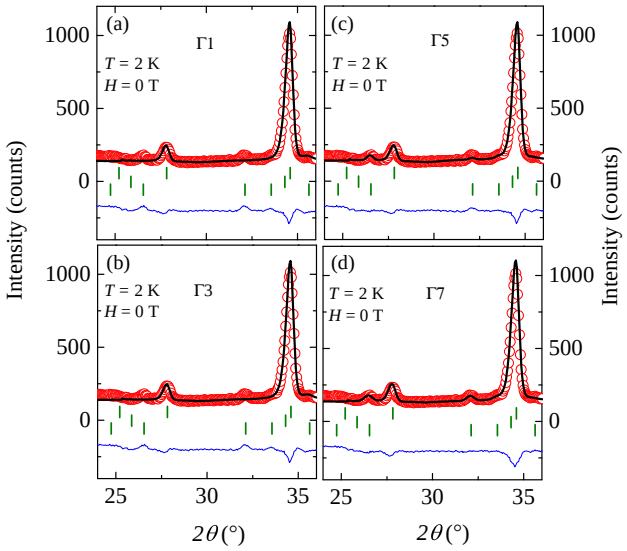

Figure 4. (color online) The refinement of diffraction patterns obtained at $T = 2$ K, $H = 0$ T in all the allowed irreducible representations, (a) Γ_1, (b) Γ_3, (c) Γ_5 and (d) Γ_7. It is clearly seen that the best fit is from Γ_7 representation.

with the application of 2 T transforms from an antiferromagnet (AFM) to that of a ferromagnet (FM). The FM spin structure for the $H = 2$ T case is shown in (d) where the net FM moment points along the crystallographic a axis. It should be noted that for random grain orientations and for magnetic moments parallel to the direction of the field, magnetic moments point to a, b, and c axes with equal probability. The refinements were performed based on the Γ_{12} representation. As such the moment direction in figure 3 (d) represents the magnetic structure for the grains with the a-axes aligned to the external magnetic field. After refining the diffraction data in the temperature range 1.5 K – 10 K, we obtain the temperature dependence of magnetic moment for both H = 0 T and 2 T, see Fig 3 (e). The magnetic phase transition at $T_N = 5.1$ K is thus confirmed. With the application of 2 T, the inflection in the order parameter shifts to $T \approx 3.5$ K below which the magnetic moment saturates to a value of 1.25 μ_B/f.u. From Fig 4 (a, b) in Ref. [[23]], we can see that upon increasing the applied magnetic field from 0.1 T to 0.8 T, the peak at $T_N = 5.1$ K shifts to lower temperature. Similarly, the isothermal magnetization at 2 K (Fig 5 in Ref. [23]) shows that the magnetic moment attained at 2 T is about 1.25 μ_B/f.u. which is comparable to the magnitude that we see from the refined magnetic moment at $H = 2$ T. From the magnetization data, we observe that the maximum magnetic moment attained by the Pr moments in PrCuSi is about 2 μ_B/f.u. at 9 T. Attempts were made to incorporate the magnetic moment of Cu in the refinement of the neutron diffraction data obtained under applied field. However, no reliable values of magnetic moment for Cu could be refined. The magnetic order parameter that is depicted in Fig 3 (e) has an abrupt change of slope in the temperature range 4-6 K which might indicate the polarization contribution of the free electrons due to the localized moments of Pr.

In Fig 5 (a, b) the temperature dependence of the lattice parameter a, c and the unit cell volume of PrCuSi are presented for both $H = 0$ T (open circles) and 2 T (filled circles). Both a and unit cell volume display anomalies at T_N. Upon application of 2 T, the cell volume increases as shown in panel (b). This is a strong indication of the presence of magnetoelastic effect upon application of magnetic field. The variation of lattice parameters display a weak anomaly below T_N in the zero field case which seems to vanish with the application of 2 T. In the case of $Pr_{0.5}Y_{0.5}Mn_2Ge_2$, anisotropic lattice parameter changes were observed at T^{Pr} (ordering of Pr sublattice) and T^{inter} (the first transition from the paramagnetic to the intralayer antiferromagnetic state) with the application of 4 T. The strong spontaneous magnetostriction was attributed to the presence of Fmc and $AFmc$ states[19]. In the canonical magnetocaloric intermetallic, $Gd_5Si_2Ge_2$ related compounds, large volume magnetostriction is found upon the application of external magnetic fields [18]. Given the recent results on the magnetostriction and magnetocaloric effects in NdCuSi and GdCuSi[16, 15], the strong magnetostructural effect is a motivating aspect to probe in detail for the presence of such effects in PrCuSi.

Shown in the panels (c) and (d) of Fig 5 are the contour plots of diffracted intensity plotted as a function of the scattering angle versus applied magnetic field, $H(T)$ at T = 1.5 K. Panel (c) shows the plot with $H(T)$ up to 5 T while a magnified plot (up to 1.5 T) is presented in (d) (for $23^\circ \leq 2\theta \leq 45^\circ$). Focusing on the panel (d), at 0 T we have the AFM magnetic ground state. At $H \approx 0.4$ T indication of development of FM reflection is obtained. In fields around $H \approx 0.8$ T a clear FM reflection (1 0 0) emerges. At the same time the AFM reflection ($\frac{1}{2}$ -$\frac{1}{2}$ 2) becomes progressively weaker and disappears. An intermediate range of mixed (AFM + FM) phase in the field range $0.4 \leq H \leq 0.8$ T is hence identified. Our analysis of the field-dependent diffraction data at 2 K (not presented) also gave similar qualitative and quantitative features as shown by the 1.5 K data.

The specific heat, $C_p(T)$, of PrCuSi reported in Ref. [23] shows a sharp anomaly at $T = 5.09$ K where the magnitude of $C_p(T)$ reaches 26.2 J/mol K. The $C_p(T)$ of the lattice analogue, LaCuSi, does not show any anomalies and hence support the fact that the magnetism in PrCuSi originates from Pr. The magnetic entropy evaluated at T_N, in the presence of zero and applied magnetic fields showed a remarkable lowering of entropy under magnetic field. For example, the entropy $S_{H=0\ T}^{T=5.1\ K} = 3.9$ J/mol K whereas $S_{H=4\ T}^{T=5.1\ K} = 2.1$ J/mol K indicate that the application of 4 T removes nearly 46% of zero field entropy at T_N. The presence of short-range fluctuations suggested directly by this observation is in full conformity with the mixed-magnetic phase scenario that we observe at $T = 1.5$ K, shown in Fig 5 (d).

Based on these findings, we sum up the magnetism of PrCuSi in the H–T phase diagram shown in Fig 6 (a). The data points in the figure are obtained from the present neutron diffraction study as well as from the previous investigation using specific heat and magnetic measurements. At $T = 1.5$ K and $H = 0$ T, PrCuSi is an antiferromagnet where the Pr moments adopt the $k(\frac{1}{2}\frac{1}{2}0)$ spin structure as depicted in Fig 3 (c) (Γ_7 representation). As the field is increased, even at a weak value of magnetic field, $\approx$

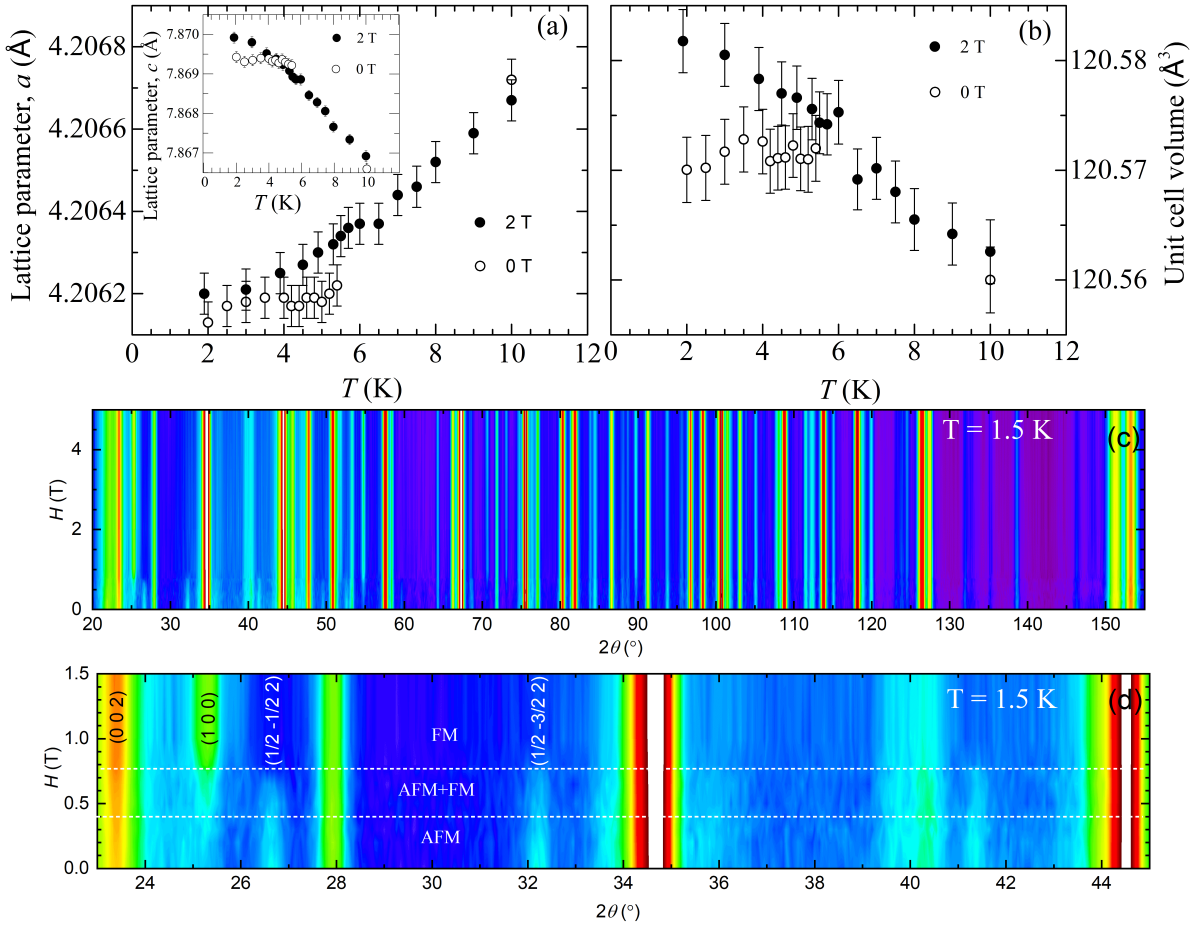

Figure 5. (color online) (a, b) Shows the temperature dependence of the lattice parameters, a, c and the unit cell volume indicating clear discontinuity at $\approx$ 5 K (T_N = 5.1 K). The panel (c) shows a color map of the diffracted intensity at T = 1.5 K plotted as a function of diffraction angle, $2\theta(^\circ)$, versus external magnetic field, $H(T)$. A magnified view is presented in (d) where the different magnetic phases that stabilize in H are indicated. Note the presence of the mixed (AFM + FM) phase.

0.8 T a ferromagnetic $k(000)$ arrangement of spins occurs as seen in Fig 3. Through the present diffraction study we obtain direct evidence for the short-range ordered mixed AFM and FM phase that exists below T_N. Data taken at H = 2 T allows us to assign the magnetic structure as a collinear FM described by Γ_{12} magnetic representation. In the phase diagram presented in Fig 6, the red circles represent the data points obtained from the maximum in $C_p(T)$ which did not change with the application of magnetic field. In the phase diagram presented in figure 6, the boundary between the AFM and the FM regions have a first-order nature. The AFM→FM transition under an applied field follows the definition of a tricritical transition [27]. Note that the critical analysis performed in the previous work by Strydom *et al.,* [23] on the specific heat data yielded an exponent $\alpha = 0.48(1)$ which is significantly close to the value of 0.5 predicted for a tricritical point using, $C_{\rm crit}(T) = A_0 + \frac{A_+}{\alpha} t_+^{-\alpha}$ [28].

Table 2 collects the magnetic parameters as reported in the literature along

Table 2. A collection of magnetic parameters for different RCuSi compounds. The crystal structure, magnetic ordering temperature (T_N), ordering wave vectors ($k_{\rm ord}$), observed and calculated spin-only magnetic moment (μ and $\mu_{\rm spin}$) and Curie-Weiss temperature (θ_p) are presented in the table.

	SG.	Type	T_N (K) T_c (K)	$k_{\rm ord}$	$\mu(\mu_{\rm B})$	$\mu_{\rm spin}(\mu_{\rm B})$	θ_p (K)	Ref.
CeCuSi	$P6_3/mmc$	Ni_2In	15.5	–	2.54	0.4	–2 K	[12]
PrCuSi	$P6/mmm$	AlB_2	14	–	3.39	3.2	8 K	[14]
PrCuSi (0 T)	$P6_3/mmc$	Ni_2In	5.1	$(\frac{1}{2}\ \frac{1}{2}\ 0)$	1.4	3.2	–4.1	This work
PrCuSi (2 T)	$P6_3/mmc$	Ni_2In	3.5	(0 0 0)	1.25	3.2	–	This work
NdCuSi	$P6_3/mmc$	Ni_2In	3.1	(0 0 0) $(\frac{1}{2}\ \frac{1}{2}\ 0)$	3.87	3.62	–11 K	[16]
GdCuSi	$P6_3/mmc$	Ni_2In	14.2 5	–	8.1	7	11.7 K	[15]
TbCuSi	$P6_3/mmc$	Ni_2In	16	$(\frac{1}{20}\ 0\ \frac{1}{2})$	8.7 (at 4.2 K)	10	–	[8]
DyCuSi	$P6_3/mmc$	Ni_2In	11.9	$(\frac{1}{30}\ 0\ \frac{1}{5})$	8.7	9	20	[29, 9]
HoCuSi	$P6_3/mmc$	Ni_2In	9.5	$(\frac{1}{15}\ 0\ \frac{1}{6})$	3.3	10	15	[29, 9]
ErCuSi	$P6_3/mmc$	Ni_2In	6.8 3.5	$(\frac{1}{12}\ 0\ 0)$	9.1	9	–	[10]
TmCuSi	$P6_3/mmc$	Ni_2In	6.5 5.8	$(\frac{1}{13}\ 0\ 0)$	6.2 (at 1.5 K)	7	–	[11]

with the of results on PrCuSi from the present work. Within the goup of RCuSi compounds adopting the Ni_2Al-type crystal structure a clear distinction can be made between the group of heavy rare-earth compounds which all adopt an incommensurate magnetic structure and the RCuSi compounds where R represents a light rare earth which adopt magnetic structures commensurate with the crystal structure. No neutron data are available for GdCuSi and hence the type of magnetic propagation vector for this antiferromagnetic compound is not known. The two different magnetic structures found for PrCuSi, *e.g.* antiferromagnetic in zero magnetic field with $k(\frac{1}{2}\frac{1}{2}0)$ and ferromagnetic with $k(000)$, correspond to those coexisting in NdCuSi in zero field [16]. The closeness to the ferromagnetic state is found as well in CeCuSi and in TmCuSi [11] where the incommensurate antiferromagnetic structure changes to a ferromagnetic as a function of temperature with a coexistence of both magnetic phases in an intermediate temperature range. The transition temperatures (T_N) show a near-linear trend with the de Gennes factor, $(g-1)^2J(J+1)$; which is plotted in Fig 6 (b). In the present case, Pr occupies a position in this plot with the lowest transition temperature. The de Gennes factor is reliable in the presence of strong spin-orbit coupling on the ion and a strong interionic exchange interaction between the spins. Previous work indicates that with the increase in the number of $4f$ electrons, the magnetic structure of RCuSi changes. For example,

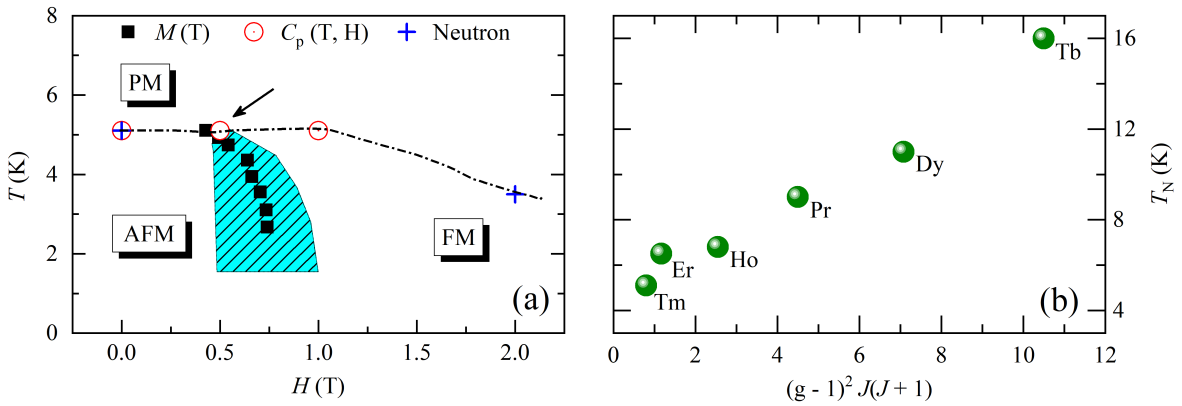

Figure 6. (color online) (a) The H–T phase diagram of PrCuSi. The mixed (AFM + FM) phase that forms below the T_N in applied fields between 0.4 T and 0.8 T is identified through the present neutron study. The high field FM phase is stabilized at weaker fields below 1 T but persists up to 9 T. The dash-dotted line is provided as a guide to eye. (b) The transition temperature, T_N of various RCuSi compounds plotted as a function of de Gennes factor.

in the case of Dy and Tb compounds, the R moment lies in the ab plane whereas for Er and Tm, the moment assumes a direction parallel to c. Among the different RCuSi compounds, only Ho and Pr in the present case seem to display an ordered moment value that is reduced compared to the theoretical value for free ion (Table 2). Crystal field effects and the local ordering of Cu and Si in these structures might significantly influence the observed ordered moment values. The layered structure of RCuSi is susceptible to stacking faults which play a role in the creation of polymorphs and distorted structures. It is interesting to note that the ordered moment of Pr in PrCuSi with AlB_2 structure is comparable to that of the free moment of Pr^{3+} (Table 2).

The PrCuSi compound prepared by Oesterreicher *et al.,* was annealed at 800 °C [14]. It crystallized in the AlB_2 structure with the $P6_3/mmm$ space group where Cu and Si appear disordered and displayed a $T_N = 14$ K. Later studies showed that a low temperature modification of the RCuSi compounds are attainable through annealing at slightly low temperatures [6]. Through annealing at 750 °C, PrCuSi was prepared in the Ni_2In-type structure where Cu and Si is well ordered. In addition to the low temperature annealing, it was understood that the ratio of the atomic radii of R to Cu influenced the type of structure that RCuSi adopted [6]. When the ratio was at 1.28, ScCuSi adopted a AlB_2-type structure whereas when the ratio was close to 1.5, LaCuSi took the Ni_2In-type ordered structure. In the present case of PrCuSi, the ratio is 1.46. This, in conjugation with the low temperature annealing can stabilize the structure in the Ni_2In-type. In our previous study [23] we did not observe the minority phase with AlB_2 structure, however, in the present case it is estimated as 4%. Although, no indication of a phase transition at 14 K is obtained through magnetic, specific heat (previous studies) or neutron scattering (present work).

4. Conclusions

Our neutron diffraction investigations on PrCuSi proves that the compound crystallizes in the ordered Ni_2In-type crystal structure with the hexagonal space group $P6_3/mmc$. In addition to this major structural phase, a minor phase of the AlB_2 phase ($P6/mmm$, 4% weight) also coexist in the material. The present work confirms an antiferromagnetic transition in the Pr lattice at $T_N = 5.1$ K. With the application of 2 T, a ferromagnetic phase is realized in PrCuSi, whereas a mixed (AFM + FM) phase in intermediate field values. Clear indications for the presence of a magnetostructural effect are obtained from the behavior of the unit cell volume upon the application of a magnetic field. Our work motivates a fresh look into the crystal and magnetic structures of other RCuSi materials especially since these materials are now being revisited for the magnetocaloric effect. Finally, we present an updated H–T phase diagram for PrCuSi combining the data points from the previous magnetization and specific heat measurements as well as current neutron diffraction data.

Acknowledgements

HSN acknowledges UTEP start-up support. CMNK acknowledges the financial support by FWF project P27980-N36 and the European Research Council (ERC Consolidator Grant No 725521). DTA acknowledges financial assistance from CMPC-STFC grant number CMPC-09108. AB would like to acknowledge DST India, for Inspire Faculty Research Grant. AMS acknowledges the SA-NRF (93549) and UJ URC/FRC for financial support.

[1] Palstra T T M, Nieuwenhuys G J, Vlastuin R F M, Van den Berg J, Mydosh J A and Buschow K H J 1987 *J. Magn. Magn. Mater.* **67** 331–342
[2] Gupta S and Suresh K 2015 *J. Alloys and Comp.* **618** 562–606
[3] Hu Z and Bao-Gen S 2015 *Chinese Physics B* **24** 127504
[4] Gupta S, Suresh K G and Nigam A K 2014 *Journal of Alloys and Compounds* **586** 600–604
[5] Rieger W and Parthé E 1969 *Monatshefte für Chemie* **100** 444–454
[6] Iandelli A 1983 *J. Less Common Metals* **90** 121–126
[7] Hovestreydt E, Engel N, Klepp K, Chabot B and Parthé E 1982 *J. Less Common Metals* **85** 247–274
[8] Bażela W, Szytuła A and Leciejewicz J 1985 *Solid State Commun.* **56** 1043–1045
[9] Schobinger-Papamantellos P, Buschow K and Ritter C 2004 *J. Alloys Comp.* **384** 12–21
[10] Schobinger-Papamantellos P, Buschow K, Duong N and Ritter C 2001 *J. Magn. Magn. Mater.* **223** 203–214
[11] Schobinger-Papamantellos P, Ritter C, Buschow K and Duong N 2002 *J. Magn. Magn. Mater.* **247** 207–214
[12] Gignoux D, Schmitt D and Zerguine M 1986 *Solid State Commun.* **58** 559–562
[13] Sondezi-Mhlungu B, Adroja D, Strydom A, Paschen S and Goremychkin E 2009 *Physica B* **404** 3032–3034
[14] Oesterreicher H 1976 *Physica Status Solidi (a)* **34** 723–728
[15] Gupta S, Suresh K and Lukoyanov A 2015 *J. Mater. Sci.* **50** 5723–5728

[16] Gupta S, Suresh K, Das A, Nigam A and Hoser A 2015 *APL Materials* **3** 066102
[17] Pecharsky V K and Gschneidner Jr K A 1997 *Phys. Rev. Lett.* **78** 4494
[18] Morellon L, Algarabel P, Ibarra M, Blasco J, Garcia-Landa B, Arnold Z and Albertini F 1998 *Phys. Rev. B* **58** R14721
[19] Wang J, Caron L, Campbell S, Kennedy S, Hofmann M, Cheng Z, Din M M, Studer A, Brück E and Dou S 2013 *Phys. Rev. Lett.* **110** 217211
[20] Wang J, Campbell S, Cadogan J, Studer A, Zeng R and Dou S 2011 *Appl. Phys. Lett.* **98** 232509
[21] Wang J, Kennedy S, Campbell S, Hofmann M and Dou S 2013 *Phys. Rev. B* **87** 104401
[22] Tomka G, Ritter C, Riedi P, Kapusta C and Kocemba W 1998 *Phys. Rev. B* **58** 6330
[23] Strydom A M 2010 *Eur. Phys. J. B* **74** 9–18
[24] Rietveld H M 1969 *J. Appl. Crystall.* **2** 65–71
[25] Rodriguez-Carvajal J 2010 *LLB, CEA-CNRS, France*
[26] Wills A S 2000 *Physica B* **276** 680–681
[27] Huang K 1987 *Statistical Mechanics, 2^{nd} Edition* ((New York: John Wiley & Sons))
[28] Riedel E and FJ W 1972 *Phys. Rev. Lett.* **29** 349
[29] Oleś A, Duraj R, Kolenda M, Penc B and Szytuła A 2004 *J. Alloys Comp.* **363** 63–67